Chapter III. Substratum stiffening promotes the quantitative, progressive loss of contact-inhibition of proliferation

Abstract

Cancer progression occurs through multiple genetic and epigenetic perturbations. Elucidating how these perturbations collectively confer selective advantages, such as unconstrained proliferation, is central to our understanding of disease progression and for developing treatment strategies. Here, we show that (1) there are measurable, quantitative degrees of contact-inhibition of proliferation, and that (2) the stiffening of the microenvironment, a widely observed perturbation during cancer development, promotes a quantitative, progressive loss of contact-inhibition. Even when substratum stiffening has no discernible effect on the phenotype of contact-inhibition, it significantly reduces the threshold amount of EGF needed to transition cells from contact-inhibited to contact-independent proliferation. Thus, the threshold amount of EGF provides a metric of the extent of contact-inhibition. Quantifying the threshold EGF level reveals the potent synergism between matrix stiffening and EGF signaling. Matrix stiffening reduces the EGF threshold by over two orders-of-magnitude, thereby markedly reducing the extent of EGF amplification needed to switch into contact-independent proliferation. These potent effects of substratum stiffening involve the erosion of cell-cell contacts, changes in nuclear compartmentation of ZO-1, and the disruption of subcellular localization of EGFR, leading to a selective effect on ERK, but not Akt, signaling. Our findings have direct implications for our understanding of multi-hit cancer progression and offer design

principles for engineering spatial patterns of growth of multicellular structures using synthetic mechanically-tunable biomaterials.

Manuscript prepared for submission by Kim. J.-H. and A. R. Asthagiri

Introduction

A hallmark of normal epithelial cells is contact-inhibition of proliferation (1). In contrast, cancer cells proliferate chaotically in a contact-independent manner, leading to tumor formation. Elucidating how epithelial cells transition from a contact-inhibited state to a contact-independent mode of proliferation will provide insight into a pivotal step in cancer progression.

Epithelial cells reside in a microenvironment replete with stimuli, and cell-cell contact is just one among many signals that regulate cell proliferation. Parsing how contact-inhibition is enforced in a rich microenvironment that also presents conflicting growth-promoting stimuli remains a challenge. Both biochemical and physical mechanisms seem to be involved. Cell-cell contacts affect GF-mediated intracellular signaling pathways, such as ERK and Akt, to suppress cell cycle progression (2-3). Further upstream, GF receptors themselves interact with receptors that mediate cell-cell adhesion, such as E/VE-cadherin (4-6). In addition, cadherins mediate contact-inhibition by mechanically coupling neighboring cells and affecting the distribution of traction forces in multicellular clusters (7). Atypical cadherin, Fat, and ERM family proteins, Merlin, and Expanded, are also implicated in the Hippo pathway which has emerged as one of the key regulators of contact-inhibition and organ size determination in both *Drosophila* and mammalian systems (8-9).

While progress continues in uncovering the physiochemical mechanisms mediating contact-inhibition, it remains unclear how these mechanisms collectively reconcile the competing influences of GFs and cell-cell contact on cell cycle activity. We recently proposed a quantitative framework for contact-inhibition in which the levels of cell-cell contact and epidermal growth factor (EGF) determine whether cell proliferation is contact-inhibited or contact-independent (Fig. 1) (10). A significant implication of the proposed state diagram is that contact-inhibition and its loss during cancer development must be viewed from a quantitative perspective. It suggests that cancer-promoting perturbations may quantitatively shift normal cells closer to the transition line to contact-independence. While the effect of such perturbations on the gross phenotype would remain latent (i.e., proliferation would still be contact-inhibited), the perturbations would have a quantitative, measureable effect on the threshold amount of EGF needed to transform cells into a contact-independent mode of proliferation. Thus, the proposition is that the "degree of contact-inhibition" may be quantified by how close a cell system is to the transition line and that the effect of multiple seemingly latent hits can be tracked by measuring changes in the EGF threshold.

Here, we set out to explore whether physiologically-relevant cancer-promoting events actually cause such measurable quantitative shifts in the degree of contact-inhibition of epithelial cells. To test this hypothesis, we focused on a key event during cancer progression: the increase in the rigidity of tumor environments (11-12). Our results demonstrate that stiffening the adhesive substratum quantitatively shifts non-transformed, contact-inhibited epithelial cells closer to the transition into a contact-

independent state. Increasing the stiffness of a collagen- or fibronectin-coated elastic substrate reduces the threshold amount of EGF needed to induce tumor-like, contact-independent proliferation. By reducing the EGF threshold, matrix stiffening reduces the extent to which EGF signaling must be amplified to enable contact-independent growth, thereby quantitatively facilitating transformation. Our findings provide quantitative insights into how matrix compliance and EGF signaling synergistically affect contact-inhibition. These insights have implications for our understanding of cancer progression and offer design principles for engineering spatial patterns and rates of growth of multicellular structures using synthetic mechanically-tunable biomaterials.

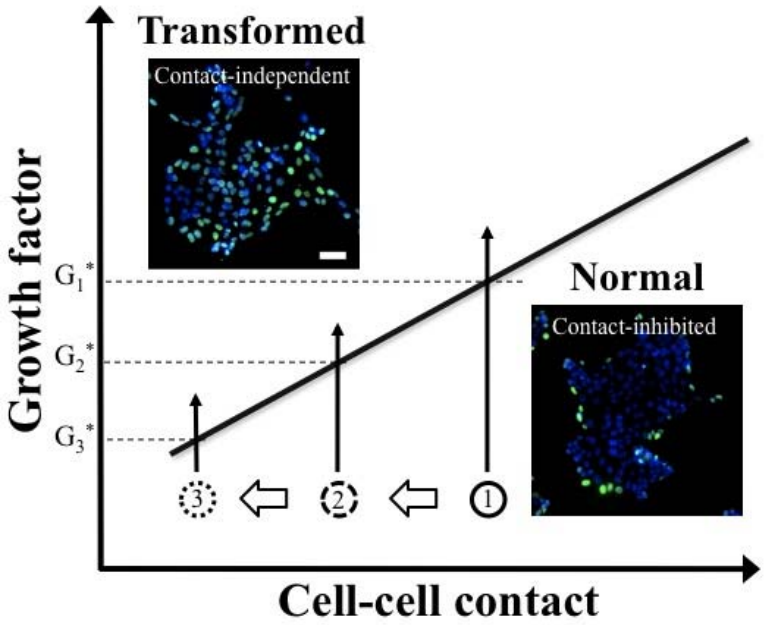

Fig. 1. State diagram for contact-inhibition of proliferation and the hypothesis of quantitative, progressive loss of contact-inhibition. Contact-inhibited cells (1)

transition to a contact-independent mode of proliferation upon crossing a critical threshold level of growth factor (G_1^*). We hypothesize that cancer-promoting perturbations may quantitatively shift normal cells closer to the transition line to contact-independence (1 → 2 → 3). Although such perturbations may not have a phenotypic effect (i.e., cells remain contact-inhibited), we hypothesize that these perturbations may have a quantitative, measurable effect on the threshold amount of EGF (G_1^* → G_2^* → G_3^*) needed to transform normal cells to achieve contact-independent growth. Insets show representative fluorescence images probed for BrdU incorporation (green) and DAPI (blue) for epithelial clusters in contact-inhibited and contact-independent states of proliferation. (Scale bar, 50 μm.)

Results

Substratum compliance affects spatial patterns in proliferation and contact-inhibition of proliferation

To explore the effect of substratum compliance on contact-inhibition of proliferation, we cultured Madin-Darby canine kidney (MDCK) epithelial cells on collagen (ColI)-coated polyacrylamide gels of varying stiffness and identical adhesion ligand composition (Fig. S1). Over a range of substratum compliance (7-31 kPa), cells formed two-dimensional multicellular clusters. On the most compliant substratum (7 kPa), treatment with a supra-saturating dose of EGF (100 ng/ml) induced BrdU uptake only at the periphery of clusters (Fig. 2Ai and B). Interior cells did not exhibit cell cycle activity on soft substrates. Increasing the stiffness of the substratum eliminated

this spatial pattern in proliferation (Fig. 2Aiii and B). Quantitative analysis showed that BrdU uptake of interior cells was equivalent to that of peripheral cells on the stiffer substrates (17-31 kPa) (Fig. 2B).

To confirm that the observed spatial pattern in proliferation on soft substrates was in fact due to contact-inhibition, we tested the effect of diminishing cell-cell interactions by down-regulating E-cadherin expression using siRNA. Compared to a control construct, transfection with siRNA reduced E-cadherin expression by ~50% in MDCK cells grown on the compliant substratum (Fig. S2). Transfection with a control siRNA had no effect on the spatial pattern in proliferation on soft substrates (Fig. 2C). In contrast, the spatial pattern was eliminated in cells treated with E-cadherin siRNA. These results demonstrate that E-cadherin-mediated cell-cell contact is involved in establishing the spatial pattern in proliferation on soft substrates.

Taken together, these observations reveal that cell-cell contact effectively inhibits cell cycle activity among interior cells on soft substrates, leading to spatial patterns in proliferation. In contrast, on stiffer substrates, cell-cell contact is not sufficient to halt cell proliferation, leading to uniform cell cycle activity throughout the multicellular cluster.

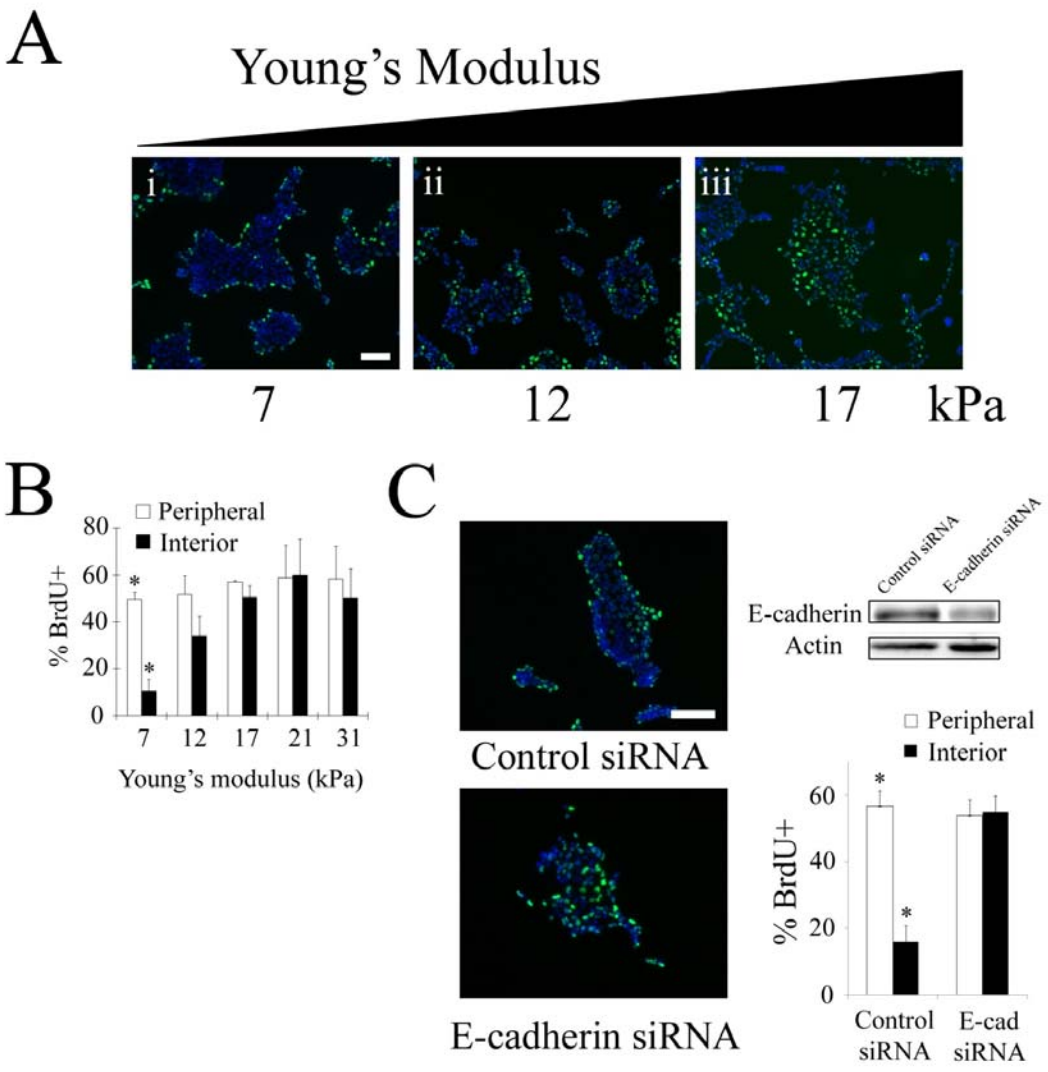

Fig. 2. Substratum compliance affects spatial patterns in cell-cycle activity and contact-inhibition of proliferation. (A) MDCK cells cultured on ColI-coated polyacrylamide gels of varying stiffness were treated with 100 ng/ml EGF following serum starvation. BrdU incorporation (green) and DAPI staining (blue) were assessed 16 h after EGF treatment. (B) The graph shows the quantitation of the percentage of peripheral and interior cells undergoing DNA synthesis. Error bars, s.d. (n = 2-5), *, $P < 0.01$. (C) The effect of down-regulating E-cadherin on spatial patterns in proliferation

induced by compliant substrata. MDCK cells grown on soft substrates were transfected with control or E-cadherin siRNA in serum-free medium for 24 h. Cells were then stimulated with 100 ng/ml EGF. BrdU uptake (green) and DAPI (blue) were assessed 16 h later. Percentage of peripheral and interior cells incorporating BrdU was quantified. The extent of knockdown in E-cadherin was determined by Western blot. Equal loading was confirmed by probing for actin. Error bars, s.d. (n = 2), *, $P < 0.01$. (Scale bars, 100 μm.)

Substratum compliance quantitatively modulates the transition between contact-inhibited and contact-independent proliferation

Our initial experiments showing the effect of substratum compliance on contact-inhibition were conducted at a single supra-saturating dose of EGF. We have previously shown that epithelial cells transition between contact-inhibited and contact-independent modes of proliferation when the amount of EGF crosses a critical threshold level (Fig. 1). Thus, we reasoned that it may be important to evaluate the effect of substratum compliance on contact-inhibition in the context of a third critical aspect of the microenvironment, soluble GFs.

To begin to examine this interplay between EGF, substratum compliance and cell-cell contact, we examined cell cycle activity in clusters of non-transformed human mammary epithelial cells (MCF-10A) cultured on substrates of different mechanical compliance and exposed to a broad range of EGF concentrations. On soft substrates (7 kPa), at the low and intermediate EGF concentrations (0.01 and 1 ng/ml EGF,

respectively), peripheral cells proliferated with a higher propensity than interior cells, exhibiting the spatially-patterned, contact-inhibited mode of proliferation (Fig. 3Ai and Aii). The fraction of interior cells undertaking DNA synthesis was approximately 2-fold lower than the fraction of cells uptaking BrdU in the periphery of the clusters (Fig. 3B). However, as the EGF concentration was increased above 1 ng/ml, the spatial disparity in proliferation diminished such that an equal fraction of interior and peripheral cells incorporated BrdU when stimulated with 100 ng/ml EGF (Fig. 3Aiii and B). These findings reveal that even on soft surfaces, both contact-inhibited and contact-independent modes of proliferation can occur and that the state of the system depends not only on substratum stiffness, but also on whether the level of EGF is above or below the threshold (in this case, ~1 ng/ml EGF).

A key question is whether this EGF threshold is sensitive to substratum compliance. That is, does changing substratum compliance quantitatively modulate the transition point between contact-inhibition and contact-independent proliferation? To address this question, we repeated the EGF dose study, now using stiffer substrates (31 kPa). As with the soft surface, we found that MCF-10A cells exhibited both contact-inhibited and contact-independent modes of proliferation. At relatively low EGF concentrations (0.001 and 0.01 ng/ml), BrdU uptake was concentrated at the periphery of clusters, exhibiting a spatial pattern in proliferation (Fig. 3Aiv and B). Upon increasing the EGF concentration above 0.01 ng/ml, the spatial pattern in cell cycle activity was eliminated (Fig. 3Av, Avi, and B). In particular, at an EGF concentration of 1 ng/ml when cells on the soft surface were contact-inhibited (Fig. 3Aii), cells on the stiff

substrate exhibited contact-independent growth with both peripheral and interior cells proliferating with equal propensity (Fig. 3Av).

These results demonstrate that substratum stiffening (from 7 to 31 kPa) quantitatively reduces the EGF threshold from 1 to 0.01 ng/ml in MCF-10A cells. Thus, growth is not simply contact-inhibited on soft substrates and contact-independent on stiff substrates. Rather, changes in substratum compliance have a quantitative effect on the degree of contact-inhibition. Matrix stiffening reduces the EGF threshold at which the system transitions from a contact-inhibited to contact-independent mode of proliferation, thereby quantitatively facilitating this transformation.

We corroborated this quantitative effect of substratum compliance in another epithelial cell system. Cell cycle activity was assessed in MDCK cell clusters, now in response to varying both substratum stiffness and EGF concentration. On soft substrates (7 kPa), MDCK cells exhibited contact-inhibition even at supra-saturating doses of EGF (100 ng/ml), suggesting that the threshold EGF is too high to attain contact-independent growth on these substrates (Fig. S3A and B). However, on substrates of intermediate stiffness (17 kPa), MDCK cells underwent a clear transition from contact-inhibited to contact-independent growth at a threshold of approximately 0.1 ng/ml EGF. Thus, stiffening the substrate reduces the EGF threshold to a physiologically-accessible level. Finally, upon further stiffening the substratum to a Young's modulus of 31 kPa, cells exhibited contact-independent proliferation for all EGF concentrations, suggesting that the threshold EGF has diminished below the range tested in our experiments.

Taken together, these results in MCF-10A and MDCK epithelial cells demonstrate that substratum stiffening quantitatively modulates contact-inhibition by reducing the EGF threshold needed to shift cells from contact-inhibited to contact-independent proliferation. In addition, the results show that epithelial cell systems can exhibit different sensitivities to substratum compliance (Fig S3C). Over the same range of substratum compliance (7-31 kPa), the EGF threshold shifted two orders-of-magnitude in MCF-10A cells. Meanwhile, in MDCK cells, the effect extended even beyond the range of EGF concentrations used in our experiments. This difference in sensitivity to substratum compliance may arise from the difference in adhesion structures between two cell types. For example, MCF-10A cells lack Crumbs3 required for the tight junction formation and full epithelial cell polarity (13).

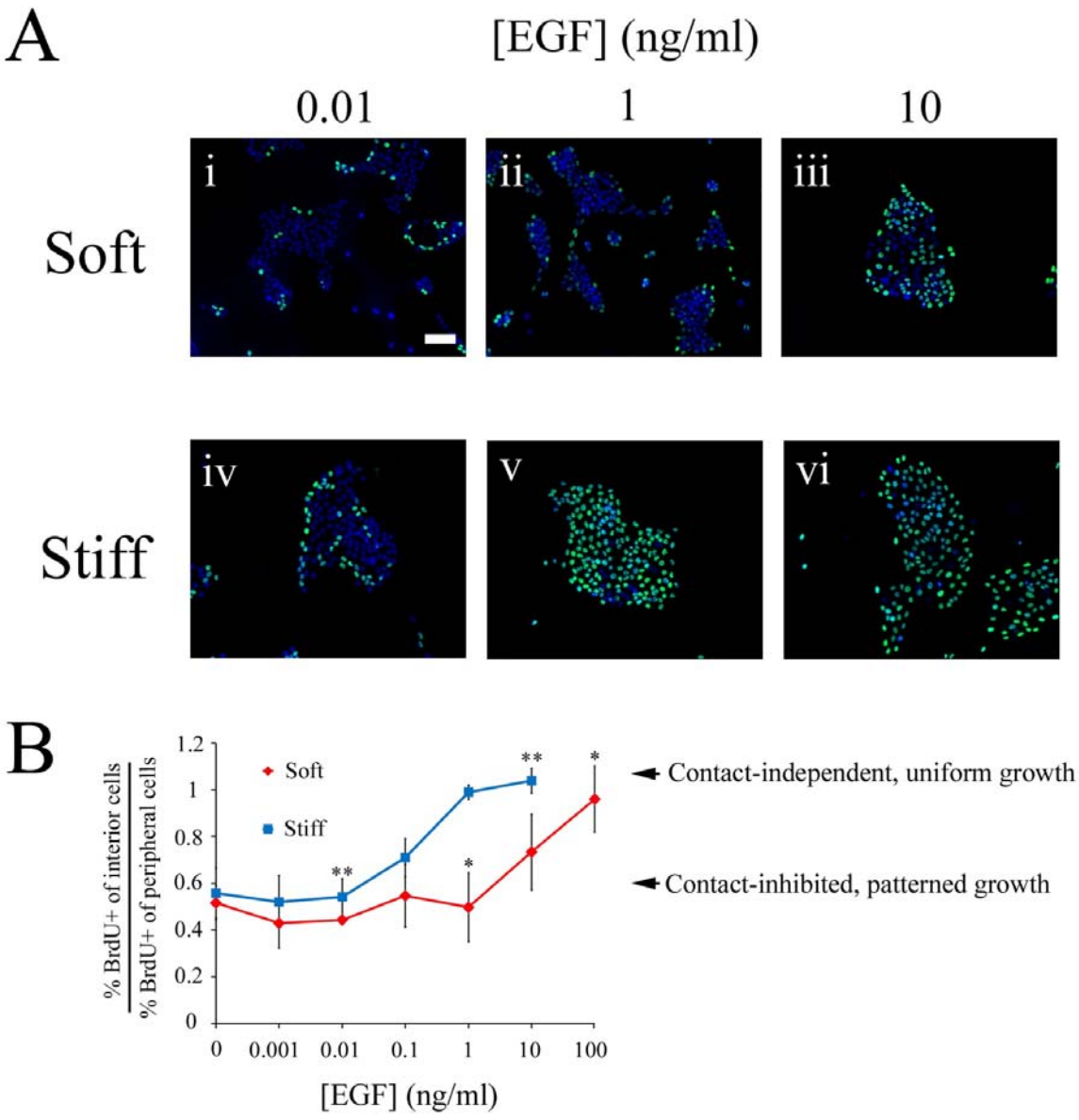

Fig. 3. Substratum stiffening reduces the EGF threshold needed to transition from contact-inhibited to contact-independent proliferation. MCF-10A cells plated on soft and stiff substrates coated with fibronectin were serum-starved for 24 h and stimulated with the indicated doses of EGF or left untreated. (A) BrdU uptake (green) and DAPI staining (blue) were assessed 22 h after EGF treatment. (B) The fractions of interior and

peripheral cells incorporating BrdU were quantified and the ratio of these two fractions is plotted as a function of EGF concentration. Error bars, s.d. (n = 2-3), * and **, $P < 0.01$. (Scale bar, 100 μm.)

Substratum compliance affects the maturation of cell-cell contacts

Our results reveal that stiffening the adhesive matrix reduces the threshold EGF at which the system transitions from contact-inhibited to contact-independent growth. This suggests that matrix stiffening may slide the cell system to the left on the state diagram (Fig. 1). That is, increasing stiffness may attenuate cell-cell contacts. To test this possibility, we examined the subcellular localization of E-cadherin and ZO-1. In mature epithelial monolayers, E-cadherin localizes typically to basolateral regions while ZO-1 is found in an apical band of mature cell-cell contacts (14).

In MDCK cells, we observed strong basolateral localization of E-cadherin at cell-cell junctions (indicated by white arrows) in cells seeded on soft substrates (Fig. 4A and B, left). In contrast, on stiff substrates, E-cadherin exhibited partial basolateral localization in addition to significant residual localization in the cytosol (Fig. 4A and B, right). These observations suggest that more mature cell-cell contacts are established on more compliant substrates.

This effect of substratum compliance on contact maturation was even more evident in the subcellular localization of the tight junction-associated protein, ZO-1. Apical localization of ZO-1 at cell-cell contacts was sharply evident in cells on soft

substrates, while only modestly present on stiff substrates (Fig. 4B). More strikingly, we observed significant differences in ZO-1 nuclear localization on soft versus stiff substrates (Fig 4B and C). On the soft surface, ZO-1 was found in the cytoplasm and nucleus only among the cells at the periphery of the cluster. The growth-arrested cells in the interior of the cluster did not exhibit nuclear ZO-1 localization. In contrast, on the stiff surface, significant nuclear localization of ZO-1 was observed among all cells in the cluster. This nuclear localization of ZO-1 was highly correlated with the proliferation patterns on soft and stiff substrates (Fig. 2). Together, these results demonstrate that increasing substratum stiffness disrupts contact maturation as evidenced by the disorganization of cell-cell junctions at a molecular level.

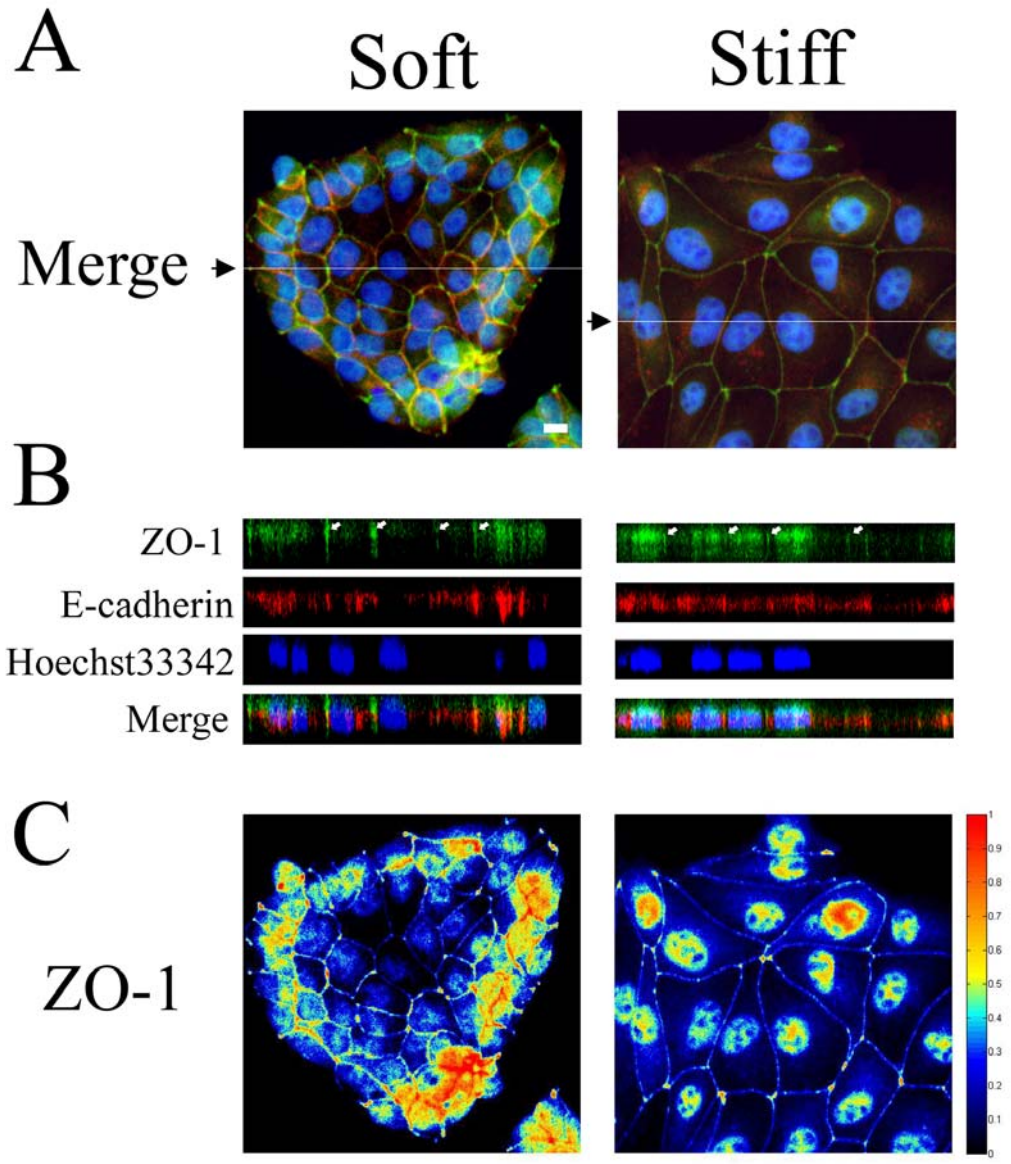

Fig. 4. Substratum compliance affects the molecular organization of adhesion structures at cell-cell contacts. MDCK cells cultured on soft and stiff substrata were serum starved for 24 h and immunostained for ZO-1 (green) and E-cadherin (red). Nuclei were co-stained with Hoechst33342 (blue). (A) Merged images were generated by projecting down in the *z*-direction so that each pixel represents the average intensity value over the *z*-stacks. White lines (pointed by black arrows) in the merged images

indicate the planes for which *x-z* section views were generated. (B) *x-z* view of the plane indicated by the white line in the merged image. White arrows indicate cell-cell contacts. (C) Heat maps of ZO-1 represent the relative abundance of the molecule within epithelial clusters across the *z*-stacks. (Scale bar, 10 μm.)

Enhanced contact-maturation on soft substrates selectively affects EGF receptor (EGFR) and ERK signaling, but not Akt signaling

The emerging model from our data is that stiff substrates disrupt cell-cell contacts and sensitize cellular response to EGF, thereby reducing the threshold EGF needed to transform the system into a contact-independent mode of proliferation. To elucidate how substratum stiffening-mediated disruption of cell-cell contacts affects EGF signaling, we examined the effect of modulating substratum compliance on the subcellular localization of EGFR. On a soft substratum, EGFR was highly localized to the basolateral membrane compartments at which stable E-cadherin-mediated adherens junctions formed (Fig. 5A, left, indicated by white arrows). In contrast, on a stiffer substratum, EGFR seemed to be evenly distributed among apical and basal membranes without co-localizing with E-cadherin (Fig. 5A, right). These results suggest that substratum stiffening may reduce the EGF threshold by disrupting cell-cell contacts and de-localizing EGFR from mature cell-cell contacts.

To determine whether this change in EGFR sequestration affects receptor signaling, we assayed the phosphorylation of EGFR on the Y1068 residue (Grb2 binding site) following 15 min of EGF stimulation at 100 ng/ml in MDCK clusters grown on soft

and stiff substrates. In contrast to the spatially uniform phosphorylation in cell clusters on the stiff substratum, both the level of EGFR phosphorylation and the formation of intracellular vesicles through EGFR internalization were diminished in the interior of cell clusters on the soft substratum (Fig. 5Bi). This spatial pattern in EGFR phosphorylation and internalization corresponds to the observed growth patterns (Fig. 2). We quantified the total cytoplasmic level of phospho-Y1068 EGFR in single cells at the periphery and interior of clusters. Consistent with our qualitative assessment, EGFR Y1068 phosphorylation was diminished in central cells by 20% relative to peripheral cells on the soft surface, but this spatial pattern was not found on the stiff substratum.

To determine whether these effects of substratum compliance on EGFR localization and phosphorylation transduce to downstream signaling pathways, we examined two EGF-mediated intercellular signals, ERK and Akt, that are involved in cell cycle regulation (15). Following 15 min of stimulation with 100 ng/ml EGF, cells were immunostained for phospho-ERK and phospho-Akt. On the soft substratum, ERK signaling was diminished by approximately 40% in the interior cells compared to their peripheral counterparts (Fig. 5Bii), correlating to the spatial pattern in EGFR phosphorylation and proliferation in this condition (Fig. 2 and 5Bi). Meanwhile, on stiffer substrates, ERK activation was homogeneous across the cell cluster, consistent with uniform patterns in both EGFR phosphorylation and proliferation. In contrast to ERK, Akt signaling was uniform within cell aggregates regardless of substratum compliance (Fig. 5Biii). Thus, substratum stiffening and the disruption of cell-cell contacts selectively enhance EGF-mediated ERK, but not Akt, signaling and thereby

eliminates the spatial disparity in proliferation, leading to contact-independent proliferation.

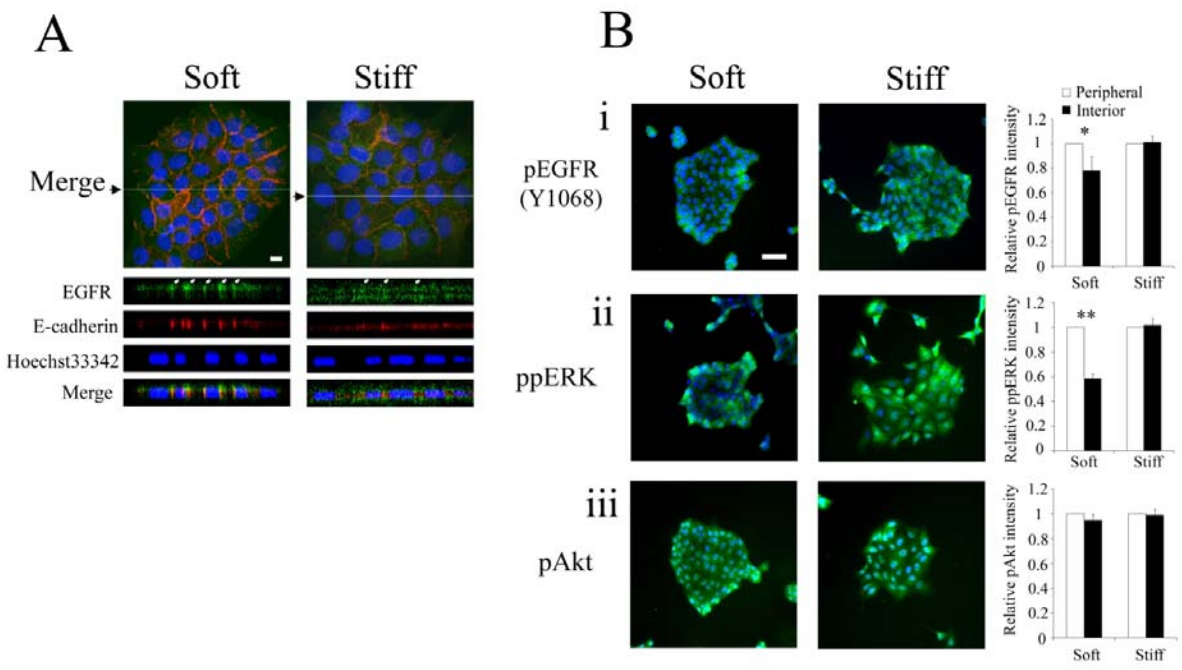

Fig. 5. Substratum compliance affects subcellular localization of EGFR and selectively regulates EGFR and ERK, but not Akt, signaling. (A) Effect of substratum compliance on subcellular localization of EGFR and E-cadherin. MCF-10A cells cultured on soft and stiff substrates were serum starved for 24 h and immunostained for EGFR (green) and E-cadherin (red). Nuclei were co-stained with Hoechst33342 (blue). Merged images represent the fluorescence signals averaged across the *z*-stacks acquired by confocal imaging. *x*-*z* views were generated at the planes indicated by white lines (pointed by black arrows) in the merged images. White arrows indicate cell-cell contacts. (Scale bar, 10 μm.) (B) Substratum compliance affects spatial patterns in EGFR and ERK, but not Akt, phosphorylation. MDCK cells plated on soft and stiff substrates were serum starved for 24 h and stimulated with 100 ng/ml EGF for 15 min.

Phosphorylation of (i) EGFR, (ii) ERK, and (iii) Akt (green) were assessed by immunofluorescence. Nuclei are labeled by staining with DAPI. The bar graphs show the relative intensities of pEGFR, ppERK, and pAkt in peripheral and central cells. Signaling intensities are reported relative to the amount of signals in peripheral cells. Error bars, s.d. ($n = 3$), *, $P < 0.05$, **, $P < 0.01$. (Scale bar, 50 μm.)

Discussion

The progressive loss of contact-inhibition: a quantitative and measurable effect of substratum stiffening

The stiffening of the tumor microenvironment is a hallmark of cancer progression (11). Here, we demonstrate that the microenvironment stiffness works synergistically with EGF signaling to regulate contact-inhibition of proliferation. We provide a framework for gauging how this interplay between mechanical and biomolecular cues in the microenvironment affects the *degree* of contact-inhibition (Fig. 1). Matrix stiffening reduces the EGF threshold that the epithelial system must cross to achieve tumor-like, contact-independent proliferation. Thus, the compliance of the microenvironment modulates how close the cellular system is to the transition line between contact-inhibited and contact-independent modes of proliferation.

The proximity of non-transformed epithelial cells to the transition line is a quantitative, measurable property of contact-inhibition. By measuring the threshold amount of EGF needed to enable contact-independent proliferation, we track

quantitatively the effect of substratum stiffening on contact-inhibition. The magnitude of the effect is significant. Increasing the elastic modulus by 4.5-fold shifts the threshold EGF nearly two orders-of-magnitude in MCF-10A cells (Fig. 3B).

This quantitative metric of contact-inhibition is an important complement to the classical qualitative perspective that normal cells are contact-inhibited while cancer cell proliferation is contact-independent. Cancer arises not from a single perturbation but from the accrual of multiple perturbations that collectively confer advantageous phenotypes, such as contact-independent proliferation. Thus, individual perturbations may have no discernible effect on gross phenotype but yet shift the system closer to a phenotypic transformation. Measuring such phenotypically latent changes in a multicellular system would give insights into how cancer-associated perturbations contribute to the complex process of transformation.

Our results reveal a metric that gauges the progressive loss of contact-inhibition. We demonstrate the utility of this metric in response to a physiologically relevant perturbation, the stiffening of substratum compliance. Unlike some genetic perturbations that produce discrete changes in the activity state of a signaling enzyme, the compliance of the microenvironment is an analog mechanical property whose magnitude may undergo graded changes during cancer progression. Our findings show that such quantitative changes in matrix compliance can modulate the degree of contact-inhibition.

The quantitative effect of substratum compliance on the EGF threshold involves the regulation of cell-cell contacts

Substratum compliance affects traction forces that isolated cells generate on the underlying substratum and the size and content of integrin-mediated focal adhesions (16). Elevated traction forces and integrin-mediated signaling in rigid environments promote proliferation (17). Furthermore, in multicellular aggregates grown on micropatterned surfaces, spatial gradients in traction forces develop across the cell cluster, corresponding to spatial patterns in proliferation (7). In this work, we focused on the effect of substratum compliance on cell-cell contacts. We observed that the quantitative effect of substratum stiffening on contact-inhibition involves the disruption of cell-cell contacts. Stiffer substrates disrupt the localization of E-cadherin and ZO-1 from cell-cell contacts. These observations on two-dimensional compliant substrates are consistent with the effects observed upon stiffening three-dimensional collagen gels and Matrigel (17), suggesting that the mechanical compliance, not the topography, of the cellular microenvironment is the principal effector of contact maturation.

Furthermore, we observed that cells on stiff substrates exhibit distinct nuclear localization of ZO-1 that correlates with the uniform, contact-independent mode of proliferation. In contrast, on soft substrates, nuclear localization of ZO-1 was observed only in the peripheral cells of a cluster, correlating with the spatial pattern in proliferation. This modulation of nuclear localization of ZO-1 by substratum compliance may be mechanistically involved in cell cycle regulation. Nuclear ZO-1 has been observed to shift to cell-cell junctions during the maturation of confluent MDCK monolayers (18),

and this event sequesters a transcription factor, ZONAB, out of the nucleus, preventing it from transcribing genes required for cell cycle activity (19).

In addition to modulating direct communication between cell-cell contacts and the nucleus, substratum compliance affected EGFR localization and downstream signaling pathways. EGFR was sequestered to the mature cell-cell contacts in cell clusters grown on soft substrates. This sequestration corresponded to reduced EGFR internalization and phosphorylation and the attenuation of ERK, but not Akt, signaling among central cells in the cluster. Similar attenuation of EGFR and ERK signaling has been observed in confluent epithelial monolayers that undergo contact-inhibition on tissue culture plastic (4). Our results demonstrate that modulating the mechanical properties of the adhesive substratum also affects contact maturation and the EGFR/ERK signaling pathways even without the spatial constraints associated with confluent epithelial sheets.

Implications for cancer treatment and tissue engineering

In conclusion, our findings demonstrate that changes in substratum compliance quantitatively modulate the degree of contact-inhibition. Stiffening the extracellular matrix moves an epithelial cell system closer to the transition to contact-independent proliferation, thereby quantitatively reducing the amount of EGF amplification needed to transform the system. Our results suggest that detecting early stages of matrix stiffening may be a particularly important diagnostic tool. During these initial stages, matrix stiffening may not render a phenotypic change but could be quantitatively pushing the

system to more easily transform. Intervening during these early stages by reducing matrix stiffness would quantitatively push the system further away from the transition point and diminish its sensitivity to molecular oncogenic signals, such as EGF. Finally, our findings provide a quantitative framework for how modulating mechanical compliance would affect spatial patterns and rates of growth of multicellular structures. This framework may facilitate the use of synthetic biomaterials whose mechanical properties may be fine-tuned, in some cases *in situ* (20), for tissue engineering applications.

Materials and Methods

Preparation and Characterization of Adhesion Ligand-coated Polyacrylamide Substrates

Polyacrylamide substrates were prepared using techniques described by Wang and colleagues (21). Substrate stiffness was manipulated by varying bis-acrylamide concentrations while keeping the acrylamide (National Diagnostic) concentration constant (10%). Type I collagen (Sigma-Aldrich) and fibronectin (Sigma-Aldrich) were covalently bound to the substrates by using a heterobifunctional cross-linker, sulfo-SANPAH (Pierce). The surface density of adhesion ligands on the substrates were examined as described in Fig. S1. Finally, Young's modulus of polyacrylamide substrates were measured by performing compression testing (22).

Cell Culture and Reagents

MCF-10A cells were cultured in growth medium as described previously (23). MDCK cells were cultured in Dulbecco's modified Eagle's medium containing HEPES and L-glutamine (Invitrogen) supplemented with 10% (v/v) fetal bovine serum (Invitrogen). For experiments, adhesion ligand-coated polyacrylamide gels bound to 25 mm circular glass coverslips (VWR) were placed in 35 mm petri-dishes (Corning), and equilibrated in growth medium for 30 min at 37°C. Then, cells were plated in growth medium for 24 h and serum starved for additional 24 h for G_0 synchronization. The following antibodies were used: anti-actin (Santa Cruz), anti-BrdU (Roche Applied Science), anti-E-cadherin (BD Transduction Laboratory), anti-EGFR, anti-phospho-Tyr1068-EGFR, anti-phospho-Thr202/Tyr204-ERK 1/2, anti-phospho-serine 473-Akt (Cell Signaling Technologies), anti-ZO1 (Zymed), DECMA-1 (Sigma-Aldrich), and Alexa dye-labeled secondary antibodies (Invitrogen). Fluorescent nuclear stains, DAPI and Hoechst33342 were obtained from Sigma-Aldrich and Invitrogen, respectively.

Knockdown Using siRNA

siRNA targeting E-cadherin and control siRNA were purchased from Ambion, and used at 50 nM. siRNA were transfected using Lipofectamine RNAiMax (Invitrogen).

Immunofluorescence and Image Acquisition

Fixed cells were permeablized, blocked, and sequentially incubated with primary and secondary antibodies. The cells were co-stained with either DAPI or Hoechst 33342, and mounted using ProLong Gold Antifade (Invitrogen). Fluorescence and confocal images were acquired using the Zeiss Axiovert 200M microscope and the Zeiss LSM 510

upright confocal microscope, respectively. The procedures followed for the quantitation of fluorescence images and reagents used for each type of stains are summarized in SI text.

Cell Lysis and Western Blot Analysis

Cell lysis and Western blot analysis were performed as described previously (23).

Acknowledgments

We thank members of the Asthagiri group for helpful discussions, Dongying Shen for her involvement in image analysis, and the Caltech Biological Imaging Center for access to the Zeiss LSM 510 upright confocal microscope. We thank J. Notbohm and G. Ravichandran for help characterizing the mechanical properties of polyacrylmaide gels. This work was supported by the Jacobs Foundation for Molecular Engineering for Medicine and the NCI Physical Sciences of Oncology Center at USC (U54CA143907).

References

1. Hanahan D & Weinberg RA (2000) The hallmarks of cancer. *Cell* 100(1):57-70.
2. Li S, Gerrard ER, Jr., & Balkovetz DF (2004) Evidence for ERK1/2 phosphorylation controlling contact inhibition of proliferation in Madin-Darby canine kidney epithelial cells. *Am J Physiol Cell Physiol* 287(2):C432-439.
3. LeVea CM, Reeder JE, & Mooney RA (2004) EGF-dependent cell cycle progression is controlled by density-dependent regulation of Akt activation. *Exp Cell Res* 297(1):272-284.
4. Curto M, Cole BK, Lallemand D, Liu C-H, & McClatchey AI (2007) Contact-dependent inhibition of EGFR signaling by Nf2/Merlin. *J Cell Biol* 177(5):893-903.
5. Lampugnani MG, Orsenigo F, Gagliani MC, Tacchetti C, & Dejana E (2006) Vascular endothelial cadherin controls VEGFR-2 internalization and signaling from intracellular compartments. *J Cell Biol* 174(4):593-604.
6. Lampugnani M, *et al.* (2003) Contact inhibition of VEGF-induced proliferation requires vascular endothelial cadherin, beta-catenin, and the phosphatase DEP-1/CD148. *J Cell Biol* 161(4):793-804.
7. Nelson CM, *et al.* (2005) Emergent patterns of growth controlled by multicellular form and mechanics. *Proc Natl Acad Sci USA* 102(33):11594-11599.
8. Hamaratoglu F, *et al.* (2006) The tumour-suppressor genes NF2/Merlin and Expanded act through Hippo signalling to regulate cell proliferation and apoptosis. *Nat Cell Biol* 8(1):27-36.

9. Yin F & Pan D (2007) Fat flies expanded the hippo pathway: a matter of size control. *Sci STKE* 2007(380):pe12.

10. Kim JH, Kushiro K, Graham NA, & Asthagiri AR (2009) Tunable interplay between epidermal growth factor and cell-cell contact governs the spatial dynamics of epithelial growth. *Proc Natl Acad Sci USA* 106(27):11149-11153.

11. Butcher DT, Alliston T, & Weaver VM (2009) A tense situation: forcing tumour progression. *Nat Rev Cancer* 9(2):108-122.

12. Levental KR, *et al.* (2009) Matrix crosslinking forces tumor progression by enhancing integrin signaling. *Cell* 139(5):891-906.

13. Fogg VC, Liu CJ, & Margolis B (2005) Multiple regions of Crumbs3 are required for tight junction formation in MCF10A cells. *J Cell Sci* 118(Pt 13):2859-2869.

14. Balkovetz DF, Pollack AL, & Mostov KE (1997) Hepatocyte growth factor alters the polarity of Madin-Darby canine kidney cell monolayers. *J Biol Chem* 272(6):3471-3477.

15. Jones SM & Kazlauskas A (2001) Growth-factor-dependent mitogenesis requires two distinct phases of signalling. *Nat Cell Biol* 3(2):165-172.

16. Discher DE, Janmey P, & Wang YL (2005) Tissue cells feel and respond to the stiffness of their substrate. *Science* 310(5751):1139-1143.

17. Paszek MJ, *et al.* (2005) Tensional homeostasis and the malignant phenotype. *Cancer Cell* 8(3):241-254.

18. Gottardi CJ, Arpin M, Fanning AS, & Louvard D (1996) The junction-associated protein, zonula occludens-1, localizes to the nucleus before the maturation and

during the remodeling of cell-cell contacts. *Proc Natl Acad Sci USA* 93(20):10779-10784.

19. Balda MS, Garrett MD, & Matter K (2003) The ZO-1-associated Y-box factor ZONAB regulates epithelial cell proliferation and cell density. *J Cell Biol* 160(3):423-432.

20. Kloxin AM, Kasko AM, Salinas CN, & Anseth KS (2009) Photodegradable hydrogels for dynamic tuning of physical and chemical properties. *Science* 324(5923):59-63.

21. Pelham RJ, Jr. & Wang Y (1997) Cell locomotion and focal adhesions are regulated by substrate flexibility. *Proc Natl Acad Sci USA* 94(25):13661-13665.

22. Franck C, Hong S, Maskarinec SA, Tirrell DA, & Ravichandran G (2007) Three-dimensional full-field measurements of large deformations in soft materials using confocal microscopy and digital volume correlation. *Exp Mech* 47(3):427-438.

23. Graham NA & Asthagiri AR (2004) Epidermal growth factor-mediated T-cell factor/lymphoid enhancer factor transcriptional activity is essential but not sufficient for cell cycle progression in nontransformed mammary epithelial cells. *J Biol Chem* 279(22):23517-23524.

Supporting Information

Quantification of immunofluorescne signals of phospho-proteins

For the quantitation of cytoplasmic pEGFR signal, cells were co-stained for E-cadherin using DECMA-1 antibody to provide a clear visualization of cell-cell contacts from the cell body. The perimeter of cell body was traced along cell-cell contacts. The area and total FITC intensity of single cell body were determined using MATLAB. The mean background intensity per pixel was also calculated for each image from the region containing no cells. This background level was multiplied by the area of the cell body and was subtracted from the total cytoplasmic FITC intensity to determine the final cytoplasmic pEGFR signal intensity for each cell.

Nuclear ppERK and pAkt signal intensities were quantified by first tracing the perimeter of each nucleus using DAPI co-staining. The area and the total FITC intensity of each nucleus were determined using MATLAB. The average background level was multiplied by the area of the nucleus and was subtracted from the total nuclear FITC intensity to determine the final ppERK or pAkt for each nucleus.

Table S1. Details of reagents used in immunofluorescence for each stain

Application	Fixation Reagents	Permeabilization	Dehydration	Blocking solution
BrdU	70% EtOH (pH 2) w/ 15 mM glycine (-20 °C)	N/A	N/A	10% goat serum + 0.1% BSA in PBS
EGFR/ZO-1/E-cadherin	Freshly prepared 4% paraformaldehyde (pH 7.4)	0.2 % Triton in PBS	N/A	Image-iT FX Signal Enhancer (Invitrogen) & 10% goat serum + 0.1% BSA in PBS
pEGFR/DECMA-1	Freshly prepared 4% paraformaldehyde (pH 7.4) + Inhibitors*	0.2 % Triton in PBS + Inhibitors*	N/A	Image-iT FX Signal Enhancer (Invitrogen) & 10% goat serum + 0.1% BSA in PBS
ppERK/pAkt	Freshly prepared 2% paraformaldehyde (pH 7.4) + Inhibitors*	0.5% NP-40 in PBS + Inhibitors*	Pure MeOH (-20 °C)	Image-iT FX Signal Enhancer (Invitrogen) & Blocking buffer**

*Phosphatase inhibitors: 1mM sodium orthovanadate, 10mM sodium fluoride, and 10mM β-glycerophosphate (all from Sigma-Aldrich)

**Blocking buffer: 130 mM NaCl, 7 mM Na_2HPO_4, 3.5 mM NaH_2PO_4, 7.7 mM NaN_3, 0.1% bovine serum albumin, 0.2% Triton X-100, 0.05% Tween-20 (all from Sigma-Aldrich), and 10% goat serum

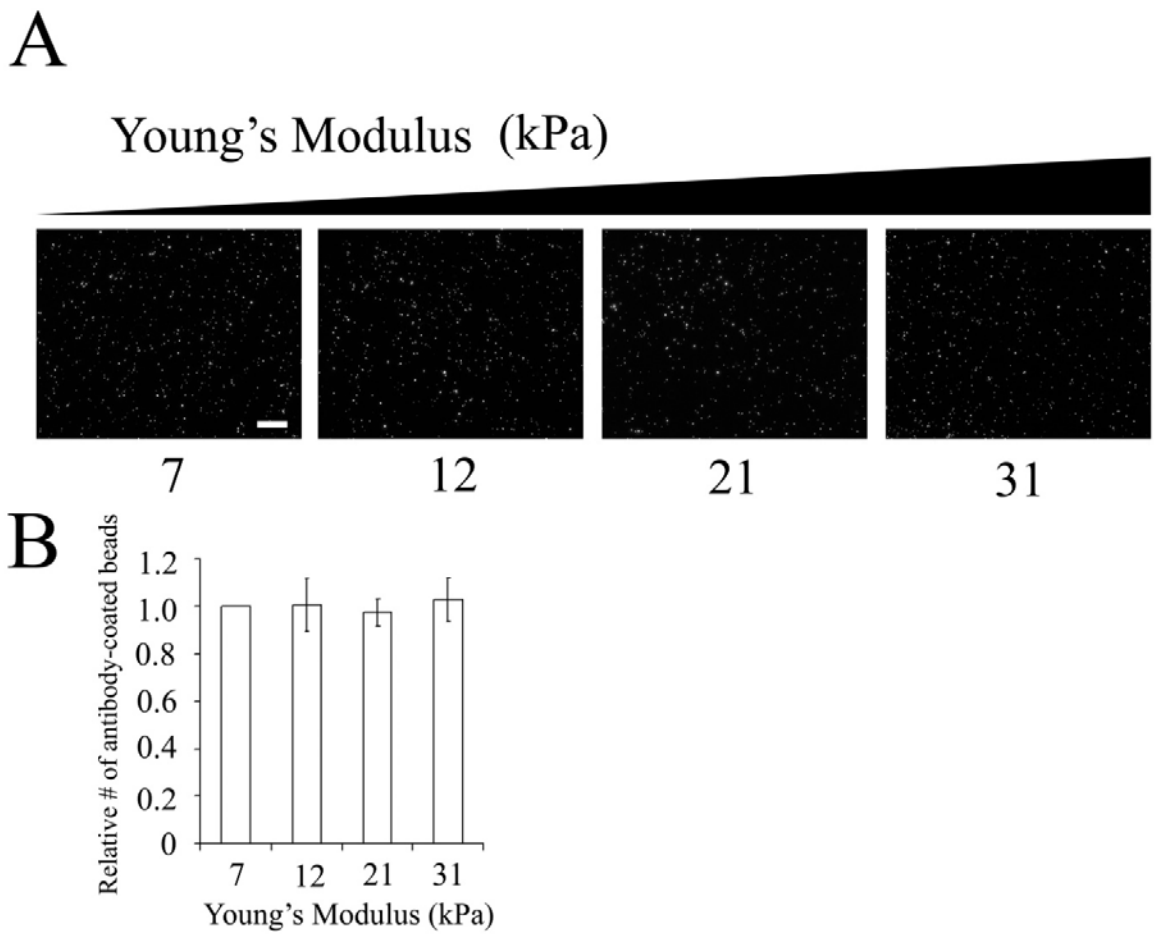

Fig. S1. Identical surface density of adhesion-ligand bound to polyacrylamide gels of varying stiffness. (A) Surface density of ColI bound to polyacrylamide gels was probed by immunofluorescence. ColI-coated substrates were sequentially incubated with anti-ColI mouse antibody (Sigma-Aldrich), and 1μm FluoSpheres® carboxylate-modified microspheres (Invitrogen) coated with anti-mouse IgG (Sigma-Aldrich). After each incubation step, the substrates were rigorously washed with PBS on the shaker multiple times. Fluorescence images of the microbeads bound to the substrate surface were acquired using the Zeiss Axiovert 200M microscope. (Scale bar, 100 μm.) (B) The

relative number of bound antibody-coated microbeads was counted at multiple image fields by using MATLAB. As a negative control, non-ColI-coated polyacrylamide gels were used and only a negligible number of microbeads was detected (data now shown). Error bars, s.d. (n = 3-4).

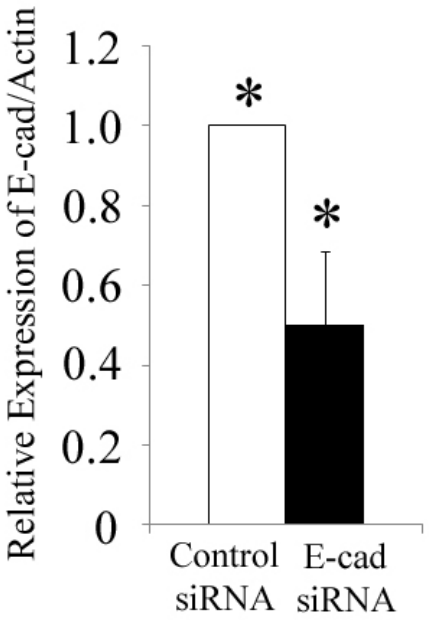

Fig. S2. Effect of siRNA treatment on E-cadherin expression. The extent of knockdown in E-cadherin was determined by quantitative Western blot analysis of relative expression of E-cadherin to actin. Error bars, s.d. (n = 3), *, $P < 0.05$.

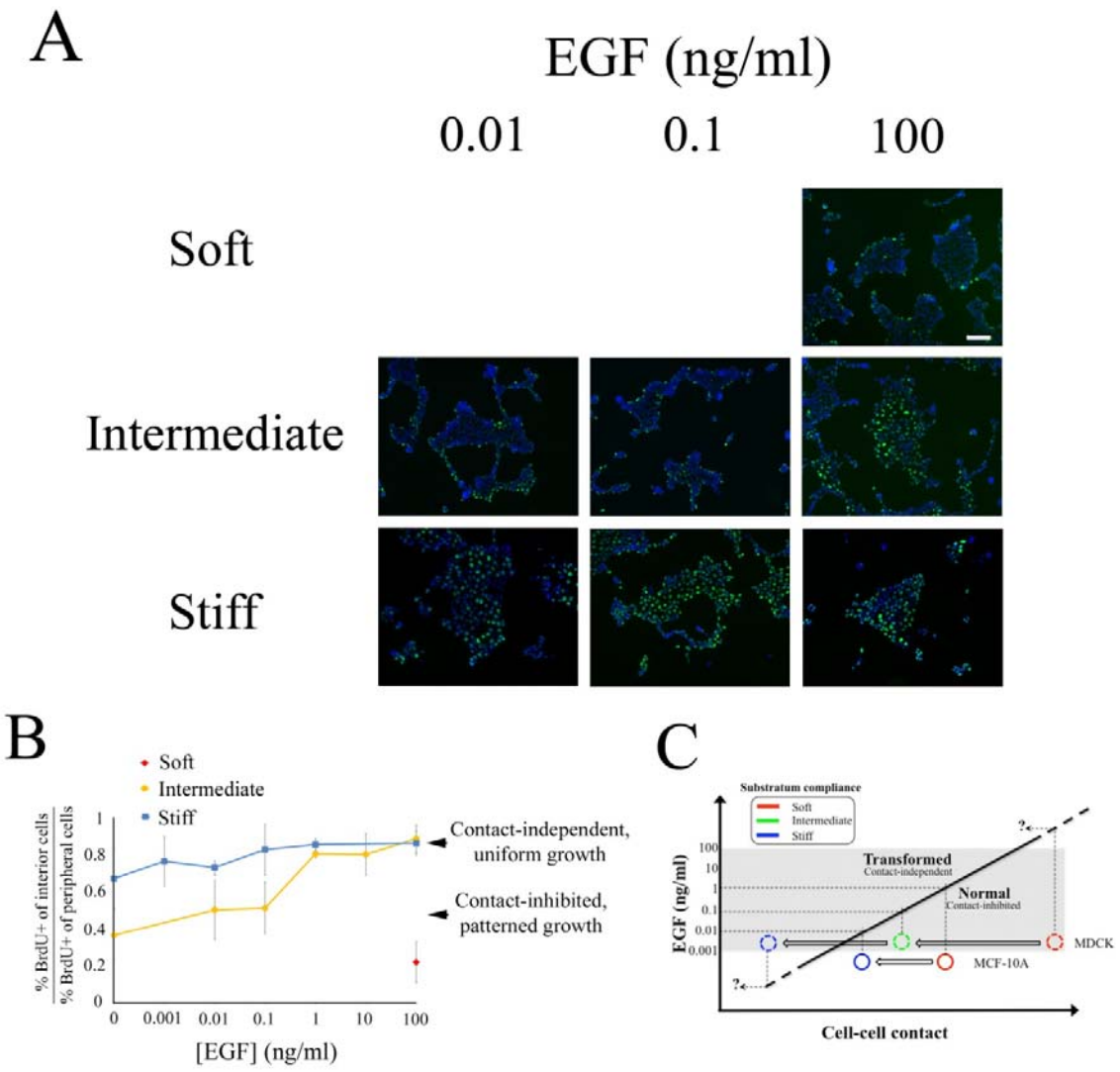

Fig. S3. The effect of substratum compliance on the threshold EGF levels for contact-inhibition. MDCK cells grown on soft, intermediate, and stiff surfaces were serum starved and stimulated with different doses of EGF. (A) BrdU uptake (green) and DAPI staining (blue) were assessed 16 h after EGF treatment. The 0.01 and 0.1 ng/ml EGF cases were not conducted for soft gels because spatial patterns in proliferation were evident even on 100 ng/ml EGF. (B) The fraction of interior cells synthesizing DNA is reported relative to the fraction of cells synthesizing DNA in the periphery of clusters. (C) Substratum stiffening quantitatively shifts the system closer to the transformed state in

both MCF-10A and MDCK cells. The two non-transormed cell lines exhibit different sensitivity to this perturbation. The shaded area in the graph refers to the range of EGF concentrations explored experimentally. MDCK on soft and stiff surfaces intersect with the transition line at a point outside of the experimentally accessible level of threshold EGF. Error bars, s.d. (n = 2), *, $P < 0.05$.